Available online at www.sciencedirect.com
ScienceDirect
Journal of Sound and Vibration 325 (2009) 240–251
JOURNAL OF SOUND AND VIBRATION
www.elsevier.com/locate/jsvi

The effect of dynamic train–bridge interaction on the bridge response during a train passage

K. Liu*, G. De Roeck, G. Lombaert

Department of Civil Engineering, K.U. Leuven, Kasteelpark Arenberg 40, B-3001 Leuven, Belgium

Received 23 September 2008; received in revised form 16 March 2009; accepted 17 March 2009
Handling Editor: C.L. Morfey
Available online 29 May 2009

Abstract

This paper investigates under which conditions dynamic train–bridge interaction should be considered for the dynamic analysis of a bridge during a train passage. The results of a moving load model are compared to those of an analysis of dynamic train–bridge interaction considering different vehicle models with a varying degree of sophistication. The effect of several parameters related to the train and the bridge is studied. The ratio of the mass of the vehicle and the bridge and the ratio of the natural frequency of the vehicle and the bridge, the train speed and the damping ratio of the bridge are identified as significant factors that determine the effect of dynamic train–bridge interaction on the bridge response.

1. Introduction

The dynamic response of railway bridges under moving trains has been a topic of research interest for many years. The basic quantity to evaluate dynamic effects due to moving traffic on bridges is the dynamic amplification factor (DAF), which represents the increase in the dynamic response with respect to the static one for a single moving load [1]. The dynamic amplification factor, however, does not take into account resonance effects due to repeated loading by a series of axles. The Eurocode 1 [1] specifies under which conditions a dynamic analysis is required.

In the dynamic analysis of the bridge, a moving train is traditionally represented as a series of moving axle loads. Timoshenko [2] developed the classical solution for a simply supported beam subjected to a moving load. An elaborate discussion of beam structures subjected to moving loads is presented by Frýba [3].

Considerable experimental and theoretical research has recently been performed on train–bridge interaction [4–7]. In the analysis of dynamic train–bridge interaction, a distinction is made between the subsystems for the train and the bridge. Both subsystems are coupled by the compatibility of displacements and equilibrium of forces at the contact points [8–10]. Different vehicle models with a varying degree of sophistication have been developed to account for the dynamic properties of the vehicle. The simplest model for a train is a series of 2 degree-of-freedom (DOF) mass–spring–damper systems that account for the suspension of the vehicle.

*Corresponding author. Tel.: +32 16 32 16 77; fax: +32 16 32 19 88.
E-mail address: kai.liu@bwk.kuleuven.be (K. Liu).

0022-460X/$ - see front matter © 2009 Elsevier Ltd. All rights reserved.
doi:10.1016/j.jsv.2009.03.021

Chu et al. [11] studied train–bridge interaction with a 3-DOF vehicle model consisting of the car body and wheel–axle sets. A time domain integration method is used to solve the dynamic equations of the coupled train–bridge system. Tan et al. [12] presented a vehicle model that has 7-DOF and is capable of accommodating both roll and pitch modes. The influence of various parameters on the behavior of the coupled system is studied in three numerical examples. Xia et al. [13] proposed a 15-DOF vehicle model and analyzed the passage of the Thalys high speed train on a concrete box–girder bridge in Antoing on the high speed line between Paris and Brussels. The model is validated by comparing the results of computations with in situ measurements.

In the literature, however, it is not very clear in which case a moving load model suffices for the prediction of the bridge response and under which conditions it is necessary to account for the dynamic interaction between the train and bridge. Liu et al. used both approaches for the particular case of the dynamic response of the Sesia viaduct during the passage of the Italian high speed train ETRY500. In this case, both approaches give predictions that are in good agreement with the experimental results [15].

The main purpose of this paper is to provide a better understanding of train induced bridge vibration and to investigate under which conditions dynamic train–bridge interaction analysis should be accounted for. It is organized in the following manner. Section 2 presents the numerical model developed for the analysis. Two methodologies are considered to represent the action of the vehicle on the bridge: (1) a moving load model and (2) a model that takes into account dynamic train–bridge interaction. In Section 3, a parametric study is performed to identify the parameters that determine the dynamic response of the bridge.

2. Numerical model

2.1. Bridge subsystem

When a finite element model of the bridge is used to study its dynamic behavior, the equation of motion of the bridge can be expressed as

$$\mathbf{M}_b\ddot{\mathbf{V}}_b + \mathbf{C}_b\dot{\mathbf{V}}_b + \mathbf{K}_b\mathbf{V}_b = \mathbf{P}_b \tag{1}$$

where $\mathbf{M}_b$, $\mathbf{C}_b$ and $\mathbf{K}_b$ are the mass matrix, damping matrix and stiffness matrix of the bridge, respectively; $\mathbf{V}_b$, $\dot{\mathbf{V}}_b$ and $\ddot{\mathbf{V}}_b$ represent the displacement, velocity and acceleration vectors of the bridge; and $\mathbf{P}_b$ is the vector with the external forces.

In the following, the modal superposition method [14] is adopted to solve the equation of motion of the bridge. It is assumed that only the first N_0 modes of the bridge are contributing to the response. The equation of motion of the bridge can be now rewritten as follows:

$$\ddot{\mathbf{q}} + \mathbf{C}_b^*\dot{\mathbf{q}} + \mathbf{K}_b^*\mathbf{q} = \mathbf{P}_b^* \tag{2}$$

where it has been assumed that the eigenvectors are normalized with respect to the mass matrix $\mathbf{M}_b$. The vector $\mathbf{q}$ collects the modal coordinates. The matrices $\mathbf{C}_b^*$, $\mathbf{K}_b^*$ and $\mathbf{P}_b^*$ are defined as follows:

$$\mathbf{C}_b^* = 2\zeta\Omega, \quad \mathbf{K}_b^* = \Omega^2, \quad \mathbf{P}_b^* = \mathbf{\Phi}^{\mathrm{T}}\mathbf{P}_b$$

where $\mathbf{\Phi}$ is the $N_0 \times N_{\mathrm{DOF}}$ matrix of eigenvectors and Ω is the $N_{\mathrm{DOF}} \times N_{\mathrm{DOF}}$ diagonal matrix of eigenvalues of the considered modes. The modal damping ratio ζ is assumed to be equal for all considered modes.

2.2. Train load modeling

The first attempt to represent the action of the vehicle on the bridge is the so-called moving load model, where the train is modeled as a series of moving loads. The force vector $\mathbf{P}_b$ can be written as follows:

$$\mathbf{P}_b(t) = \mathbf{P}_b^{qs}(t) = \sum_{i=1}^{n} \mathbf{y}_i(t)F_{Gi} \tag{3}$$

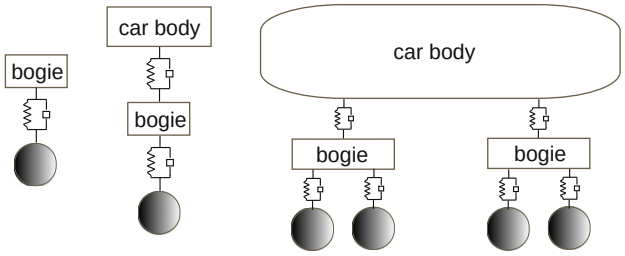

Fig. 1. (a) a 1-DOF (b) a 2-DOF and (c) a 3-DOF vehicle model for dynamic train–bridge interaction analysis.

where the superscript qs in $\mathbf{P}_b^{qs}(t)$ refers to the fact that only the quasi-static loading of the bridge is accounted for. The vector $\mathbf{y}_i(t)$ is the $N_{\mathrm{DOF}} \times 1$ vector that transfers a moving unit load to nodal loads according to the position of the ith axle. The load amplitude F_{Gi} is equal to the weight of the ith axle of the train.

To account for the dynamic effect of the train on the bridge, vehicle models with a varying degree of sophistication are considered (Fig. 1). Vehicle model c is an elaborate model that considers both the vertical motion of the car body and the bogie, while vehicle models a and b are simplified versions of vehicle model c.

In a similar way as for the bridge, the equation of motion of the vehicle can be written as

$$\mathbf{M}_v\ddot{\mathbf{V}}_v + \mathbf{C}_v\dot{\mathbf{V}}_v + \mathbf{K}_v\mathbf{V}_v = \mathbf{P}_v^{dy} \tag{4}$$

where $\mathbf{M}_v$, $\mathbf{C}_v$ and $\mathbf{K}_v$ are the mass, damping and stiffness matrices; $\mathbf{V}_v$, $\dot{\mathbf{V}}_v$ and $\ddot{\mathbf{V}}_v$ are the displacement, velocity and acceleration vectors of the vehicle system; and $\mathbf{P}_v^{dy}$ is the force vector that collects the dynamic force on the vehicle [15].

The coupling of the vehicle and bridge subsystems by the compatibility of the displacements at the contact points is now illustrated for the case of vehicle model c [15]. The equation of motion of the vehicle can be derived from the dynamic force equilibrium (Fig. 2).

The mass matrix of the vehicle can be expressed as

$$\mathbf{M}_v = \mathrm{diag}[M_1, M_2, M_1] \tag{5}$$

where M_1 and M_2 are the mass of the bogie and the car body, respectively.

The stiffness matrix of the vehicle system is expressed as

$$\mathbf{K}_v = \begin{bmatrix} 2K_V + K_{VV} & -K_{VV} & 0 \\ -K_{VV} & 2K_{VV} & -K_{VV} \\ 0 & -K_{VV} & 2K_V + K_{VV} \end{bmatrix} \tag{6}$$

where K_V and K_{VV} are the spring stiffness coefficients of the primary and secondary suspension system, respectively.

The damping matrix is derived from the stiffness matrix by replacing the stiffness coefficients (K_V, K_{VV}) by the damping coefficients (C_V, C_{VV}) of the primary and secondary suspension system.

The displacement vector $\mathbf{V}_v$ is expressed as

$$\mathbf{V}_v = [V_1, V_2, V_3]^{\mathrm{T}} \tag{7}$$

where V_1 and V_3 are the vertical displacements of the front and back bogie, respectively, while V_2 is the vertical displacement of the car body.

The force vector $\mathbf{P}_v^{\mathrm{dy}}$ is expressed in terms of the displacements and velocities of the wheel sets:

$$\mathbf{P}_v^{\mathrm{dy}} = \begin{bmatrix} K_V(V_{W1} + V_{W2}) + C_V(\dot{V}_{W1} + \dot{V}_{W2}) \\ 0 \\ K_V(V_{W3} + V_{W4}) + C_V(\dot{V}_{W3} + \dot{V}_{W4}) \end{bmatrix} \tag{8}$$

where V_{Wi} and $\dot{V}_{Wi}$ ($i = 1,2,3,4$) represent the displacement and velocity of the ith wheel set, respectively.

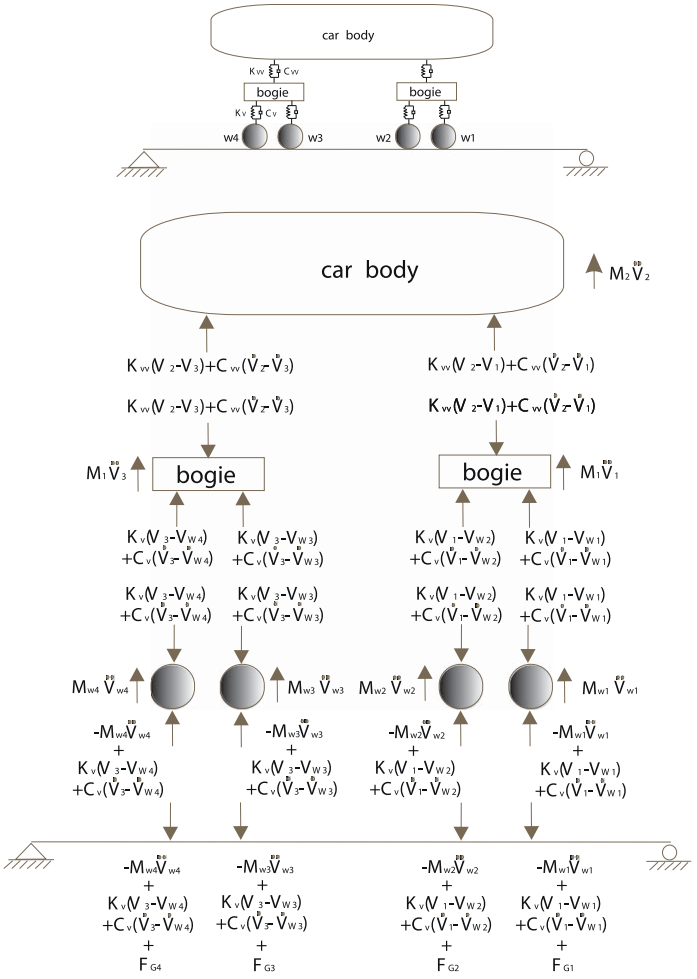

Fig. 2. A simply supported beam subjected to a moving vehicle.

With vehicle model c, the force $\mathbf{P}_b$ transferred to the bridge can be written as

$$\mathbf{P}_b(t) = \mathbf{P}_b^{\mathrm{qs}}(t) + \mathbf{P}_b^{\mathrm{dy}}(t) = \sum_{i=1}^{4} \mathbf{y}_i(t) F_{Gi} + \sum_{i=1}^{4} \mathbf{y}_i(t)(-M_{Wi}\ddot{V}_{Wi} + K_V(V_j - V_{Wi}) + C_V(\dot{V}_j - \dot{V}_{Wi})) \tag{9}$$

where $\mathbf{P}_b^{\mathrm{qs}}(t)$ and $\mathbf{P}_b^{\mathrm{dy}}(t)$ are referred to as the quasi-static and the dynamic part of the force, respectively; $\ddot{V}_{Wi}$ $(i = 1,2,3,4)$ represents the acceleration of the ith wheel set; V_j $(j = 1|_{i=1,2},\ j = 3|_{i=3,4})$ represents the displacement of the bogie and M_{Wi} and F_{Gi} $(i = 1, 2, 3, 4)$ represent the mass and the axle load of the ith wheel set, respectively.

The equations of motion are integrated according to the Newmark-β method with values $\beta = 0.25$ and $\gamma = 0.5$ corresponding to the trapezoidal rule [18]. The integration procedure is described more elaborately in Ref. [15].

3. Parametric study

For simply supported bridges, the results of ERRI D214 showed that resonance is unlikely for spans longer than 40 m [16]. This study has been limited, however, to the case of simply supported bridges of relatively short span without consideration of transverse effects. The simply supported bridge in Ref. [17] is chosen as the

Table 1
The dynamic characteristics of the Italian ETR500Y high speed train.

Item	Unit	Locomotive	Passenger car
Mass of the car body (M_2)	kg	55,976	34,231
Mass of the bogie (M_1)	kg	3896	2760
Mass of the wheel set (M_w)	kg	2059	1583
Vertical stiffness of the primary suspension system (K_V)	kN/m	1,792,200	808,740
Vertical damping of the primary suspension system (C_V)	kN s/m	15,250	7500
Vertical stiffness of the secondary suspension system (K_{VV})	kN/m	472,060	180,554
Vertical damping of the secondary suspension system (C_{VV})	kN s/m	36,250	16,250
Carriage length (d)	m	19.7	26.1

reference case in the present parametric study. The characteristics of the bridge are as follows. The bridge has a length L of 34 m, a mass per unit length $m_b = 11400\,\mathrm{kg/m}$, a bending stiffness $EI = 9.92 \times 10^{10}\,\mathrm{N\,m^2}$, and a modal damping ratio ζ of 2% for all considered modes. The fundamental natural frequency $f_b = 4.01\,\mathrm{Hz}$.

The train type considered in this study is the Italian ETR500Y high speed train. The main characteristics of the train are listed in Table 1. It is composed of a locomotive followed by eight passenger cars and another locomotive. The length of the locomotive is 19.7 m, while the length of the passenger cars is 26.1 m. The average static axle loads for the locomotives and passenger cars are 176.4 and 112.9 kN, respectively. The natural frequencies of the car body and the bogie can be estimated from the following equations:

$$f_{vc} = \frac{1}{2\pi}\sqrt{\frac{2}{\frac{1}{Kvv}+\frac{1}{2Kv}}{M_2}} \tag{10}$$

$$f_{vb} = \frac{1}{2\pi}\sqrt{\frac{2Kv + Kvv}{M_1}} \tag{11}$$

The values for K_V and K_{VV} of ETR500Y are used to estimate the frequencies of the car body and the bogie as 0.49 and 4.06 Hz, respectively.

In order to investigate the conditions under which dynamic train–bridge interaction needs to be taken into account, a parametric study is performed. The following dimensionless parameters are defined: the speed parameter α, the frequency parameter κ and the mass parameter γ. Apart from these parameters, the influence of the bending stiffness EI and the modal damping ratio of the bridge ζ is investigated as well.

The dimensionless speed parameter α is defined as

$$\alpha = \frac{v}{f_b d} \tag{12}$$

where v is the train speed, d is the characteristic length of a car and f_b is the fundamental natural frequency of the bridge. The critical speed caused by a long series of regularly spaced axles is reached at $\alpha = 1$. For the Italian high speed train ETR500Y, the characteristic length $d = 26.1\,\mathrm{m}$, so that with a value of $f_b = 4.01\,\mathrm{Hz}$ for the fundamental natural frequency, the critical speed is reached at 377 km/h.

The dimensionless frequency parameter κ is

$$\kappa = \frac{f_v}{f_b} \tag{13}$$

where f_v and f_b are the frequency of the vehicle and the first bending frequency of the bridge, respectively. Due to the low value of the natural frequency f_{vc} of the car body, this part of the vehicle is dynamically uncoupled from the bridge. Therefore the natural frequency f_{vb} of the bogie is considered for f_v in Eq. (13). For the train and the bridge in the current study $f_{vb} = 4.06\,\mathrm{Hz}$ while $f_b = 4.01\,\mathrm{Hz}$, so that the value of κ is 1.01 in the reference case.

The dimensionless mass parameter γ is defined as

$$\gamma = \frac{M_v}{M_b} \tag{14}$$

where M_v is the total mass of the train and M_b is the mass of the bridge. With $M_v = 445,544\,\text{kg}$ and $M_b = 387,600\,\text{kg}$, the value of γ is therefore 1.1495 in the reference case.

3.1. Influence of the speed parameter on the dynamic response of the bridge

According to Eurocode 1 [1], the frequency range considered in the determination of the maximum deck acceleration should have an upper limit of 30 Hz or 1.5 times the frequency of the first eigenmode of the structural element being considered. The frequency range should at least include the first three modes. For the present bridge with a fundamental natural frequency of 4.01 Hz, the threshold for low-pass filtering is therefore 30 Hz.

Figs. 3 and 4 present the dynamic amplification factor DAFu and the maximum vertical acceleration at mid-span, respectively, as a function of the dimensionless speed parameter α. The dynamic amplification factor DAFu is defined as

$$DAFu = \frac{u_{dyn}(l/2)}{u_{sta}(l/2)}$$

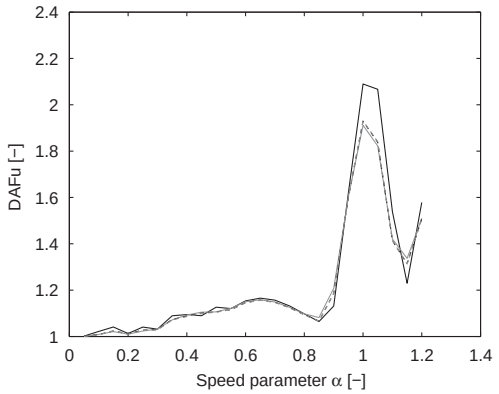

Fig. 3. The dynamic amplification factor DAFu as a function of the dimensionless speed parameter α for the moving load model (solid black line), vehicle model a (solid gray line), vehicle model b (dashed black line) and vehicle model c (dashed gray line).

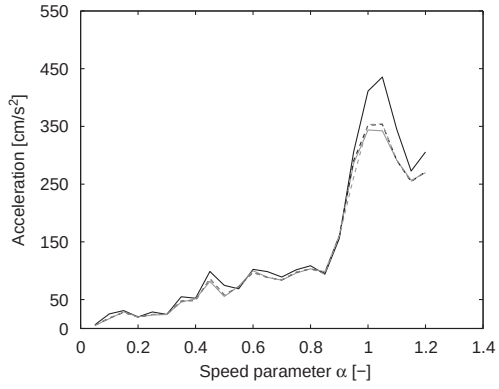

Fig. 4. Maximum vertical acceleration at mid-span as a function of the dimensionless speed parameter α for the moving load model (solid black line), vehicle model a (solid gray line), vehicle model b (dashed black line) and vehicle model c (dashed gray line).

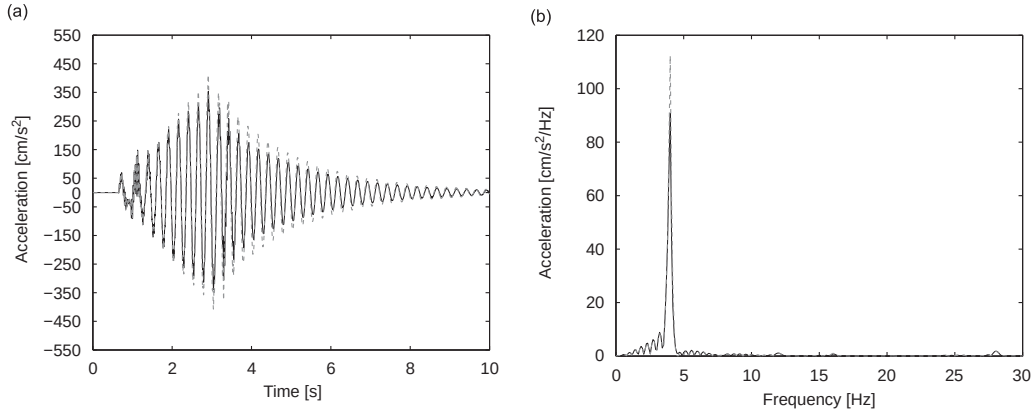

Fig. 5. (a) Time history and (b) frequency content of the acceleration at mid-span of the moving load model (dashed gray line) and vehicle model c (solid black line).

where $u_{dyn}(l/2)$ is the maximum dynamic displacement and $u_{sta}(l/2)$ is the maximum static displacement at mid-span of the bridge.

For low values of α, there is no significant difference between the different train load models. The difference, however, gets larger when the speed parameter α approaches a value of 1, which corresponds to the resonant speed. In general, the moving load model produces the largest dynamic amplification, while the vehicle models a, b and c generate a lower dynamic amplification. This is due to the presence of the suspension system which results in a reduction of the contact force applied to the bridge.

Fig. 5 depicts the acceleration at mid-span in the time domain and frequency domain for a train passage at resonant speed for the moving load model and vehicle model c. In both models, a peak occurs at 4.01 Hz, which corresponds to the first bending frequency of the bridge. A reduction of the peak magnitude is observed when dynamic train–bridge interaction is taken into account.

3.2. Influence of the frequency parameter on the dynamic response of the bridge

The dynamic train–bridge interaction is affected by the natural frequencies of the two subsystems. In the following, the stiffness of the suspension system is modified to investigate the influence of the frequency parameter κ in the range from 0.1 to 2.0.

Figs. 6 and 7 show the dynamic amplification factor DAFu and the acceleration, respectively, at resonant speed as a function of the frequency parameter κ. When the value of the parameter κ is close to 0, there is a small difference between the moving load model and vehicle models a, b and c. Due to the low stiffness of the suspension system, the vehicle is dynamically uncoupled from the bridge and the static load is the only component that affects the response of the bridge. In this case, a moving load model satisfactorily represents the vehicle. In the case where the stiffness of the suspension system is relatively high, corresponding to a high value for κ, the train can be represented by a moving mass. It is also observed that when the natural frequency of the vehicle is slightly higher than the natural frequency of the bridge, the dynamic response of the bridge at resonant speed reaches its minimum value when dynamic train–bridge interaction is accounted for.

3.3. Influence of the mass parameter on the dynamic response of the bridge

A modification of the vehicle mass changes both the quasi-static force and the dynamic force and therefore affects the dynamic response of the bridge. In this subsection, the response of the bridge to a moving train is considered for different values of the mass parameter γ between 0.1 and 3.

The parameter γ is modified by changing the mass of the vehicle, while the stiffness of the suspension system is adjusted correspondingly to maintain a constant value of 1.01 for the frequency ratio κ.

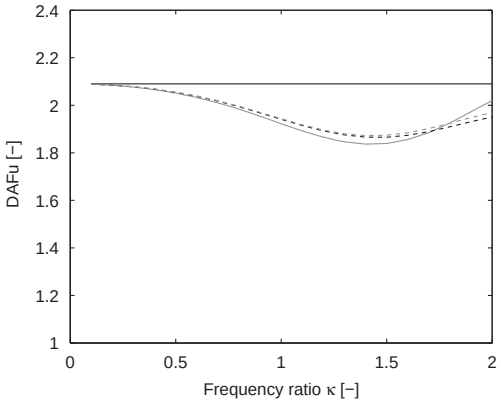

Fig. 6. The dynamic amplification factor DAFu at resonant speed as a function of the dimensionless frequency parameter κ for the moving load model (solid black line), vehicle model a (solid gray line), vehicle model b (dashed black line) and vehicle model c (dashed gray line).

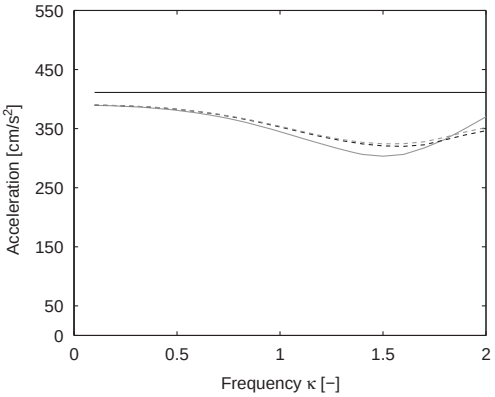

Fig. 7. Maximum vertical acceleration at mid-span at resonant speed versus dimensionless frequency parameter κ for the moving load model (solid black line), vehicle model a (solid gray line), vehicle model b (dashed black line) and vehicle model c (dashed gray line).

Figs. 8 and 9 show that the dynamic response increases linearly with the increase of the mass ratio γ for the moving load model. For low values of the mass parameter, there is a small difference between the three vehicle models and the moving load model. With an increasing mass ratio, however, dynamic train–bridge interaction becomes more important, and reduces the dynamic amplification factor DAFu. Fig. 9 shows that for a mass parameter γ of 3, the acceleration at mid-span is reduced by 32% by dynamic train–bridge interaction.

3.4. *Influence of the bending stiffness of the bridge on the dynamic response of the bridge*

A parametric study is carried out to investigate the effect of the bending stiffness of the bridge on the dynamic response of the bridge. The stiffness of the suspension system of the vehicle is adjusted so that both dimensionless parameters κ and γ have a constant value. Two additional values of $0.5EI$ and $2.0EI$ are considered for the bending stiffness of the bridge.

Figs. 10 and 11 show the dynamic amplification factor DAFu and the maximum acceleration, respectively, at resonant speed as a function of the speed parameter α for the three values of the bending stiffness. As has been observed previously, dynamic train–bridge interaction hardly affects the dynamic response of the bridge at low values of the speed parameter α. At resonant speed ($\alpha = 1$) the response is reduced in a similar way for the three values of the bending stiffness of the bridge.

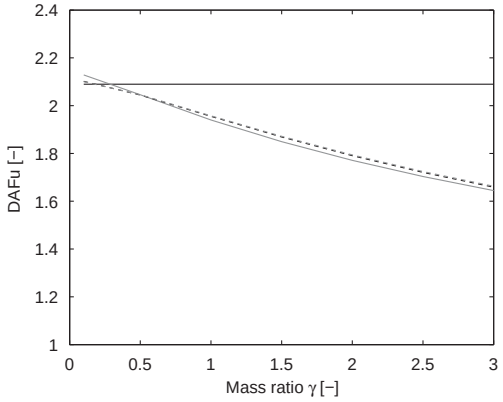

Fig. 8. The dynamic amplification factor DAFu at resonant speed as a function of the dimensionless mass parameter γ for the moving load model (solid black line), vehicle model a (solid gray line), vehicle model b (dashed black line) and vehicle model c (dashed gray line).

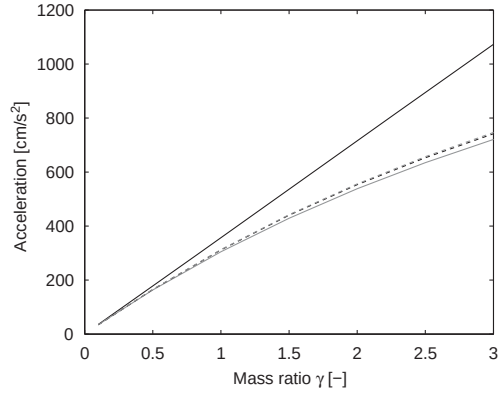

Fig. 9. Maximum vertical acceleration at mid-span at resonant speed as a function of the dimensionless mass parameter γ for the moving load model (solid black line), vehicle model a (solid gray line), vehicle model b (dashed black line) and vehicle model c (dashed gray line).

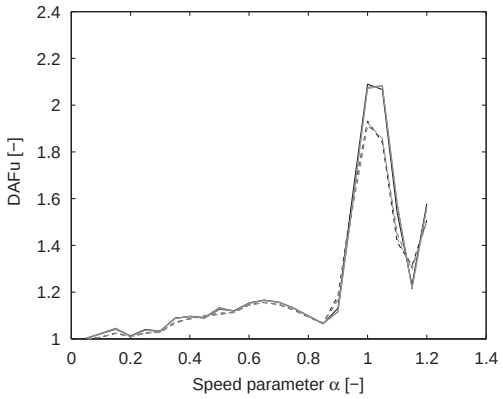

Fig. 10. The dynamic amplification factor DAFu as a function of the speed parameter α for the moving load model (solid line) and vehicle model c (dashed line) with a bending stiffness for the bridge of $1.0EI$ (black line), $0.5EI$ (thin gray line), and $2.0EI$ (thick gray line).

3.5. *Influence of the damping ratio on the dynamic response of the bridge*

In this subsection, the influence of the modal damping ratio of the bridge is analyzed. The following values of the modal damping ratio ζ are considered: $\zeta = 1\%$, 1.5%, 2%, 2.5% and 3%.

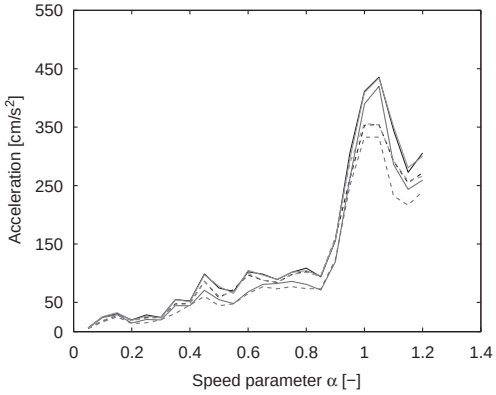

Fig. 11. Maximum vertical acceleration at mid-span as a function of the speed parameter α for the moving load model (solid line) and vehicle model c (dashed line) with a bending stiffness for the bridge of $1.0EI$ (black line), $0.5EI$ (thin gray line), and $2.0EI$ (thick gray line).

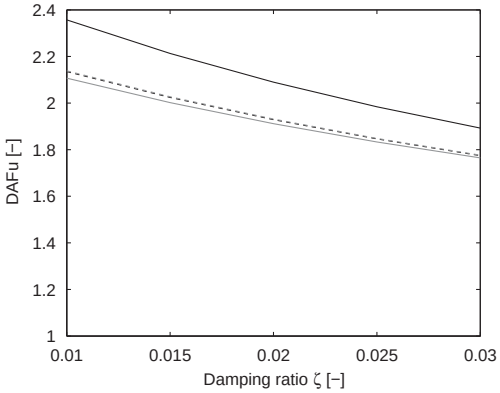

Fig. 12. The dynamic amplification factor DAFu as a function of the damping ratio ζ for the moving load model (solid black line), vehicle model a (solid gray line), vehicle model b (dashed black line) and vehicle model c (dashed gray line).

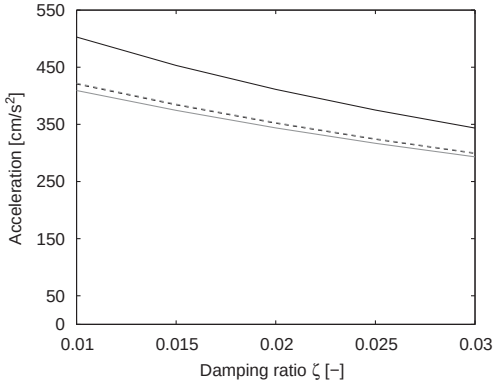

Fig. 13. Maximum vertical acceleration at mid-span as a function of the damping ratio ζ for the moving load model (solid black line), vehicle model a (solid gray line), vehicle model b (dashed black line) and vehicle model c (dashed gray line).

The influence of the damping ratio on the dynamic response of the bridge is shown in Figs. 12 and 13. As expected, an increase in the modal damping ratio of the bridge results in a reduced magnitude of the response. Moreover, an increase of the bridge damping ratio leads to a decrease of the effect of dynamic train–bridge interaction.

4. Conclusions

This study investigates the effect of dynamic train–bridge interaction on the bridge response during a train passage. The influence of several dynamic characteristics of the train and the bridge on the dynamic response of the bridge is studied. The following conclusions can be drawn from this study:

1. The dynamic amplification attains its maximum value at a critical train speed where the passage of a series of regularly spaced axles excites the bridge at its resonance frequency.
2. When the train speed approaches its critical value, dynamic train–bridge interaction results in a lower dynamic response of the bridge as compared to the moving load model. The reduction is larger for the bridge acceleration at mid-span than for the corresponding displacement.
3. When the ratio of the natural frequency of the vehicle and the bridge is much smaller than one, the response of the bridge can be estimated by a moving load model. For an increasing ratio, dynamic train–bridge interaction becomes more important and reduces the dynamic amplification at the critical speed. The largest reduction is found when the natural frequency of vehicle is slightly larger than the natural frequency of the bridge.
4. The results are dependent on the type of vehicle model and it is therefore important to choose a suitable vehicle model in the analysis. Among the vehicle models adopted in the study, vehicle models b and c give the most accurate prediction, while vehicle model a provides a good approximation due to the very low value of the natural frequency of the car body.
5. Dynamic train–bridge interaction is more important for the situation when the ratio of the mass of the vehicle and the bridge is relatively large. When the mass ratio is low, a moving load model is sufficient for the dynamic analysis of the bridge. With an increasing mass ratio, the effect of dynamic train–bridge interaction becomes more important.
6. A larger value of the modal damping ratio results in a lower dynamic response of the bridge.

Acknowledgments

The research is conducted in the framework of the EC Research Fund for Coal and Steel RTD Project RFSR-CT-2006-00032 ''DETAILS'' (design for optimal life cycle costs (LCC) of high speed railway bridges by enhanced monitoring systems). The support of the EC is gratefully acknowledged.

References

[1] EN 1990:2002/A1:2005, Eurocode—Basis of structural design, Final Draft, European Committee for standardization, CEN, 2006.
[2] S.P. Timoshenko, *History of the Strength of Materials*, D. Van Nostrand Co., 1953.
[3] L. Frýba, *Vibration of Solids and Structures under Moving Loads*, Thomas Telford, 1999.
[4] Y.K. Cheung, F.T.K. Au, D.Y. Zheng, Y.S. Cheng, Vibration of multi-span bridges under moving vehicles and trains by using modified beam vibration functions, *Journal of Sound and Vibration* 228 (1999) 611–628.
[5] H. Xia, Y.L. Xu, T.H.T. Chan, Dynamic interaction of long suspension bridges with running trains, *Journal of Sound and Vibration* 237 (2000) 263–280.
[6] C.H. Lee, M. Kawatani, C.W. Kim, N. Nishimura, Y. Kobayashi, Dynamic response of a monorail steel bridge under a moving train, *Journal of Sound and Vibration* 294 (2006) 562–579.
[7] N. Zhang, H. Xia, W.W. Guo, Vehicle–bridge interaction analysis under high-speed trains, *Journal of Sound and Vibration* 309 (2008) 407–425.
[8] C.W. Kim, M. Kawatani, K.B. Kim, Three-dimensional dynamic analysis for bridge–vehicle interaction with roadway roughness, *Engineering Structures* 19 (1997) 936–944.
[9] M.K. Song, H.C. Nohb, C.K. Choi, A new three-dimensional finite element analysis model of high-speed train–bridge interactions, *Engineering Structures* 25 (2003) 1611–1626.
[10] C.H. Lee, C.W. Kim, M. Kawatani, N. Nishimura, T. Kamizono, Dynamic response analysis of monorail bridges under moving trains and riding comfort of trains, *Engineering Structures* 27 (2005) 1999–2013.
[11] K.H. Chu, C.L. Dhar, V.K. Garg, Railway-bridge impact: simplified train and bridge model, *Journal of the Structural Division* 105 (1979) 1823–1844.
[12] G.H. Tan, G.H. Brameld, D.P. Thambiratnam, Development of an analytical model for treating bridge–vehicle interaction, *Engineering Structures* 20 (1998) 54–61.

[13] H. Xia, N. Zhang, G. De Roeck, Dynamic analysis of high speed railway bridge under articulated trains, *Computers & Structures* 81 (2003) 2467–2478.
[14] A.K. Chopra, *Dynamics of Structures: Theory and Applications to Earthquake Engineering*, Prentice-Hall, Englewood Cliffs, NJ, 2000.
[15] K. Liu, E. Reynders, G. De Roeck, G. Lombaert, Experimental and numerical analysis of a composite bridge for high-speed trains, *Journal of Sound and Vibration* 320 (2009) 201–220.
[16] ERRI D214 RP9, Railway Bridges for Speed up to 350 km/h; dynamic loading effects including resonance, Final Report, European Railway Research Institute Subcommittee D21, 1999.
[17] R. Karoumi, Response of Cable-Stayed and Suspension Bridges to Moving Vehicles, Ph.D. Thesis, 1998.
[18] N.M. Newmark, A method of computation for structural dynamics, *Journal of Engineering Mechanics* 96 (1970) 593–620.